sEMG BASED INTENTION IDENTIFICATION OF HUMAN BODY MOVEMENT RESEARCH ON ASSISTIVE ROBOT

SHUANG GU[1], YONG YUE[1], CHENGDONG WU[2], CARSTEN MAPLE[1], DAYOU LI[1], BEISHENG LIU[1]

Abstract. Recently, the robot technology research is changing from manufacturing industry to non-manufacturing industry, especially the service industry related to the human life. Assistive robot is a kind of novel service robot. It can not only help the elder and disabled people to rehabilitate their impaired musculoskeletal functions, but also help healthy people to perform tasks requiring large forces. This kind of robot has a broad application prospect in many areas, such as medical rehabilitation, special military operations, special/high intensity physical labour, space, sports, and entertainment. Assistive robots are required to autonomously identify human's movement intention in order to provide adequate support. Research carried out focus on using muscle surface electro as a clue for intention identification [1–2]. However an advanced real-time operating system is needed for integrating the existing approaches with assistive robot control. Moreover, for autonomous intention identification, a formulation of neural network will need to be developed for establishing connections between surface electro signals and human movement intentions. In this paper, a neural network based human movement intention identification method is proposed. sEMG (Surface Electromyography) signal of muscles will be processed through a novel wavelet decomposition method and then be used as input signals to a neural network which identifies human intentions. Based on human intentions, adequate support will be given to the human elbow by a real-time QNX control system. Firstly, sEMG of Palmaris longus, brachioradialis, flexor carpiulnaris and biceps brachii are analysed with a wavelet transform method. Then, the absolute variance of 3-layer wavelet coefficients is distilled, and regarded as signal characteristics to compose eigenvectors. The eigenvectors are input data of a neural network classifier used to identify 5 different kinds of movement patterns including wrist flexor, wrist extensor, elbow flexion, forearm pronation, and forearm rotation. Finally, a human arm elbow movement intention control experiment study is carried out in the QNX control system which has been established. The assistive robot can move according to the intention of the operator's action and achieve good effect. The control algorithm is straightforward and real-time, using the QNX operating system. Experimental results verify the effectiveness and advancement of the proposed algorithm.

Key words: surface electromyography; wavelet; neural network; QNX real-time system; assistive robot; motion identification.

[1] University of Bedfordshire, Department of Computer Science and Technology, Park Square, Luton LU1 3JU, UK

[2] Northeastern University, School of Information Science and Engineering, Shenyang, Liaoning, China

Rom. J. Techn. Sci. – Appl. Mechanics, Vol. 57, N^{os} 2–3, P. 217–233, Bucharest, 2012

1. INTRODUCTION

Assistive robots are a novel type of service robot and represent a high level of integration of robotics, ergonomics, control engineering, sensor technology, communications and signal processing. Assistive robots are designed for human limb power augmentation and have potential applications for elderly people, handicapped, care-workers, soldiers and firemen. There has been increased attention of research to assistive robots [3–8], and well-known systems include BLEEX [9] of Berkeley University and the Japan University of Tsukuba HAL system [10].

Robots reflect human long-held desire, for a machine, instead of people, which can engage in a variety of activities [11]. Assistive robots belong to the kind of human machine that the main function is to extend the human body function, and to amplify human power. It can not only help the elderly people and handicapped participate in the daily life, such as walking, but also be suitable for stroke patients to complete their normal rehabilitation training so as to achieve an auxiliary healing effect. For a healthy person, an assistive robot can share normal tasks as bearing of weights, handling of goods and it can also assist large tasks requiring forces several times of one's own body weight, hence reducing the labour intensity. It can also provide people with force compensation and reduce the energy consumption of the people themselves. For those who have unusual sports behaviour, an assistive robot can provide auxiliary equipment and treatment based on orthopaedic features such as scheduled robot gait behaviour with users, thus completing corrective synchronous movement of the gait.

On the other hand, from the point of view of the development of military equipment, soldiers have gradually transferred from handling battlefield weapons into being the core of a comprehensive weapon system. Through the close relationship between assistive robot and its user, soldiers can distribute equipment weight to its steel structure, thus transferring the load from the soldiers to the robot. This, potentially, can assist soldiers in loading shells, in long distance strikes, in the movement to carry the wounded and strengthen muscles and mobility, speed, endurance, action and load capacity. Assistive robots can also reduce the energy consumption of the soldiers, maximally keeping their fitness, and multiplied combat troops to fight against the enemy.

Myoelectric signals can reflect human’s intention of movements [12]. sEMG (Surface Electromyography) [13] topography is a novel method of visualizing the distribution of myoelectric signals during dynamic motion. sEMG topography provides a comprehensive examination and contraction coordination insight into the fundamental muscular strategies. The purpose of this study is to assess the feasibility of sEMG topography as an assessment tool in rehabilitation [14–18].

Numerous active units are disseminated by the series of electrical potentials of active unit motion when muscles are excited. These series of electrical potentials spread along fibre and are filtered by the volume conductor which is made of skin and fattiness. And the electrode detector set on the surface of skin finally picks up these series of electrical potentials. The signals which are got by the electrode detector both in time and space compose the sEMG.

In recent years, much work has been done with the wavelet transforming method. The features are evaluated from several selected frequency bands of the signal. Wavelet transformation represents different patterns of sEMG signal and improves the accuracy of signal classification. Blouin *et al.* [19] investigated the relations between the control of arm movement and sEMG signals through monitoring hand stableness during trunk rotation. Pal and Kumar [20] made a prediction of wavelet transformation before neural network classification. Zhang [21] used wavelet transformation to analyse sEMG, which was simulated with a fuzzy neural network method. This method could decrease the error of classification. In addition, a frequency amplifier is used to process sEMG, as the input of the artificial neural network (ANN) classification. The support vector machine (SVM) method has become prevalent. It can be based on the structural risk minimisation principle to automate the learning process. The structure model based on the statistical learning theory has a strong generalisation. The classification precision can converge to a globally optimal solution. SVM techniques are successfully used for pattern recognition and classification in the analysis of biological information. For example, Begg [22] put forward a SVM method to distinguish the gait of young people and old people and used neural network techniques to process gait information of time distance, kinematics and dynamics of a total of 24 gaits. This method can automatically identify the gait of the young/old people and can compare the adaptive level of two classifiers. Experimental results show that the SVM is suitable for gait analysis such as recognition of gait characteristics of young and old people. Osamu Fukuda [23] etc. proposed a human-assisting manipulator teleoperated by sEMG and arm motions. The proposed method can realise a new master-slave manipulator system that uses no mechanical master controller. Phongchai Nilas [24] developed an innovative human-robot communication paradigm for people with disability using sEMG via a Personal Digital Assistant (PDA). Wondae Ryu [25] etc. designed the control system which makes possible that 1 DOF manipulator replicate the wrist movements by estimating the wrist joint angle continuously from sEMG signals measured from the four muscles. This methodology can be applied to improve the control strategy for tele-operated robotic manipulator. Kim *et al.* [26] use sEMG signals and joint motion information to estimate multi-joint stiffness which can be applied to contact tasks where torque measurement is unavailable. In their

approach, an artificial neural network is trained for modelling the simplified central nervous system hierarchy. The weights of the connections between nodes are updated through standard Levenberg-Marquardt algorithm. Experiment results reported the joint stiffness of shoulder and elbow can be estimated accurately with the enhancement of joint motion information such as joint angle and velocity. However, the movement intention of humans, which could be the key to the success of task implementation, is not considered. Another challenge to the majority of the existing approaches is the experiments are often implemented through simulation. This could cause potential failure in the transportation to the real environments.

The main task in this paper is to build muscle signal acquisition system and the research in the application of assistive robots. The main part of the experiment is the design of circuit, the frequency gain testing and muscle signals acquisition on QNX operation platform. Firstly, multi-channel sEMG acquisition system is designed and the muscle signals are acquired through the amplification notch filter links. Palmaris longus, brachioracialis, flexor carpi ulnaris and biceps brachii are analysed with wavelet transform. The variance of absolute value of 3 layers wavelet decomposition coefficients are distilled, which regarded as signal characteristics to compose eigenvector. The absolute value of the wavelet coefficient is extracted as the characteristic matrix. The variance of wavelet coefficients are extracted which compared to the singular value method. Secondly, the characteristic matrix is brought into the neural network, which selected by the appropriate number of hidden nodes through training identification actions. The neural network classifier is the input to identify different 5 kinds of movement patterns including wrist flexor, wrist extensor, elbow flexion, forearm pronation and forearm rotation. Finally, the robot joint of assistive robot is designed by Solidworks software and the electrical torque linear model is established. It is the most important that the assistive robot compliant joints get the sEMG through the sensor signals for the perceived force of human muscle movements. The sEMG is used as the input of the assistive robot to perform tasks of daily life according to the human user's intention as shown in Fig. 1. The experiments of human elbow flexion and stretched out are based on the torque simulation which the results show the effectiveness of the model.

In this paper, an experimental platform for assistive robot control, which is required one of the most important parts, is established, and a recognition experiment of the assistive robot compliant joint intention is performed. Most research has been done on a computer system without a good real-time operating system. This work is based on the QNX operating system which is a real-time and multi-tasking system.

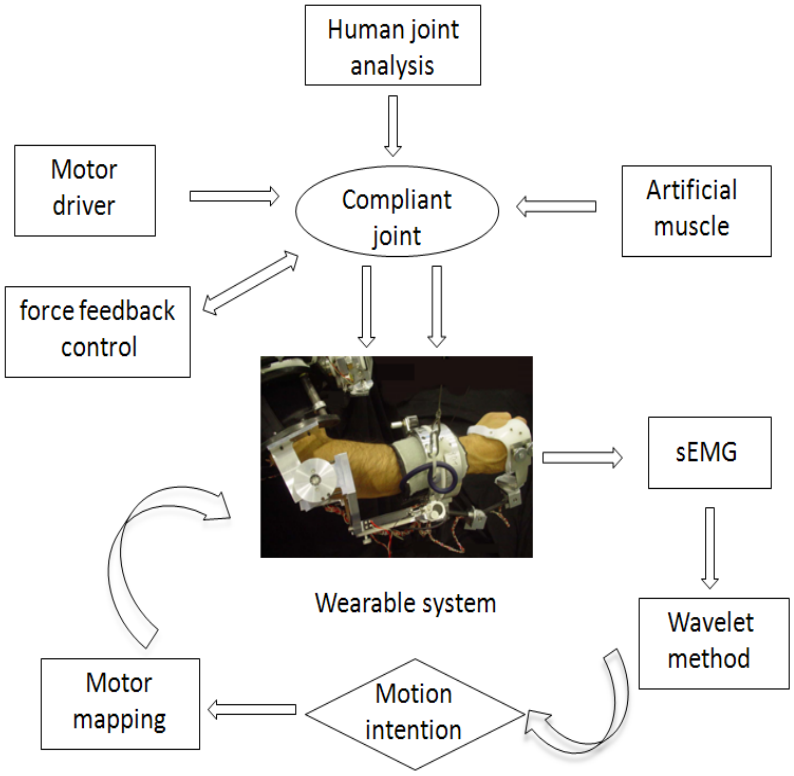

Fig. 1 – The structure of the task.

2. THEORY AND METHOD OF WAVELET TRANSFORM

In continuous wavelet transforms (CWT), a given signal of finite energy is projected on a continuous family of frequency bands (or similar subspaces of the L^p function space $L^2(R)$. L presents spaces which are function spaces defined using natural generalisations of p-norms for finite-dimensional vector spaces. They are sometimes called Lebesgue spaces, named after Henri Lebesgue; $p = 2$ is the space of square-summable sequence, which is a Hilbert space. R presents real vector space.). For instance the signal may be represented on every frequency band of the form $[f, 2f]$ for all positive frequencies $f > 0$. Then, the original signal can be reconstructed by a suitable integration over all the resulting frequency components. The frequency bands or subspaces (sub-bands) are scaled versions of a subspace at scale 1. This subspace in turn is in most situations generated by the shifts of one generating function $\Psi(t) \in L^2(R)$, the mother wavelet. For the example of the scale one frequency band [1, 2] this function is:

$$\Psi(t) = 2\,\mathrm{sinc}(2t) - \mathrm{sinc}(t) = \frac{\sin(2\pi t) - \sin(\pi t)}{\pi t}, \quad (1)$$

where $\hat{\Psi}(w)$ is Fourier transformation of the basic wavelet, $\hat{\Psi}(0) = 0$. Suppose, function family $\{\Psi_{a,b}(t)\}$ is named analysis wavelet. The subspace of scale a or frequency band $[1/a, 2/a]$ is generated by the functions (sometimes called child wavelets):

$$\Psi_{a,b} = \frac{1}{\sqrt{a}}\Psi\left(\frac{t-b}{a}\right) \quad a, b \in R, a \neq 0, \quad (2)$$

where $\Psi(t)$ is named basic wavelet, a is positive and defines the scale and b is any real number and defines the shift. Suppose $f(t)$ is a L^2 dimensional function. The continuous wavelet transformation of function $f(t)$ is defined as:

$$Wf(a, b) = \langle f, \Psi_{a,b} \rangle = \int_{-\infty}^{+\infty} \Psi_{a,b}(t) f(t)\, dt. \quad (3)$$

Suppose $f(k), k = 0, 2, \ldots, N-1$ is a discrete sequence of instantaneous rotational speed signal $f(t)$. $f(n)$ is an approximation of $f(t)$ when $j = 0$. It is marked as $c_{0,k}$. Then the discrete binary wavelet decomposition coefficient $d_{j,k}$ of signal $f(t)$ can be calculated by the following recursion formula:

$$\begin{cases} c_{j,k} = \sum_n C_{j-1,n} h_{n-2k} \\ d_{j,k} = \sum_n d_{j-1,n} g_{n-2k} \end{cases} \quad k = 0, 1, 2, \ldots, N \quad 1, \quad (4)$$

where $c_{j,k}$ is the projection of signal $f(t)$ on scale j. $d_{j,k}$ is the orthogonal projection of signal $f(t)$ in the wavelet space. h_{n-2k} and g_{n-2k} are specula direction filters. They have the following relationship with scale function $\varphi(t)$ and wavelet function

$$\Psi(t): h_0(k) = \langle \Phi_{10}, \Phi_{0k} \rangle, h_1(k) = \langle \Psi_{10}, \Psi_{0k} \rangle. \quad (5)$$

Discrete signal $c_{0,k}$ is finally decomposed to $d_1, d_2, \ldots, d_j$ (wavelet coefficients) and c_j (scale coefficient) by decomposing on scale $1, 2, \ldots, j$. They comprise difference frequency information from a high frequency to a low frequency of signal. Meanwhile they also comprise time information of the signal.

Choosing a basic wavelet function plays an important part in dealing with the signal. Most commonly, the wavelet transform function [27] comprises Harr wavelet, Daubechies wavelet, Biorthogonal wavelet and Coiflet wavelet.

Wavelet transformation has a periodic characteristic and self time-frequency. The substance of wavelet transformation is that it decomposes information from different original frequency signals which are then shown in the time axis. That is not only reflects the characteristic of the time-region of signal, but also the characteristic of the frequency-region. Meanwhile, a small scale transformation comprises a high-frequency signal, and a large scale transformation comprises a low-frequency signal. To deal with signal validly, a different scale of transformation can be selected to describe the characteristics of the signal.

The coefficient of the wavelet of each grade scale can comprise an eigenvector. Each variance of eigenvector represents a stable of the eigenvector. When the element of the eigenvector is changes slightly, the variance of the eigenvector changes slightly as well. Consequently, this reflects the information and characteristics of the eigenvector.

3. A BACK-PROPAGATION (BP) NEURAL NETWORK APPROACH

This paper employs a 3-layer BP neural network classifier. The neural network comprises an input layer, a hidden layer and an output layer. There are 12 nodes in the input layer and 5 nodes in the output layer. An S function is adopted as the transformation function for the hidden layer and a linear function as the transformation function for the output layer. The network structure is shown in Fig. 2.

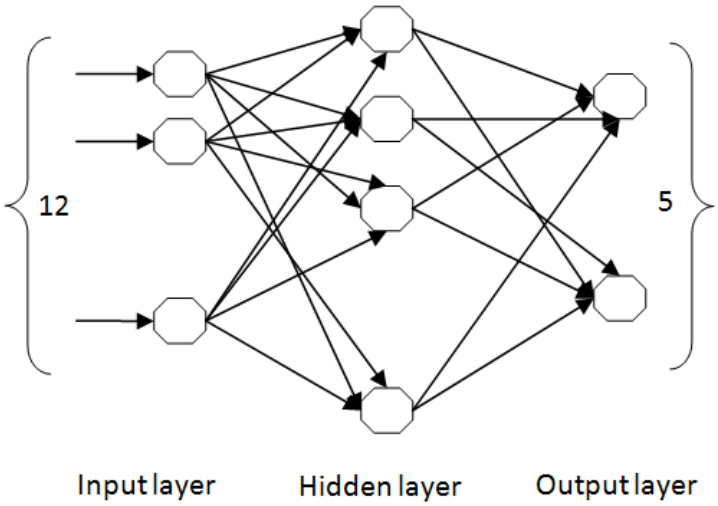

Fig. 2 – BP neural network structure.

The inputs to the neural network are 12 eigenvectors extracted from the surface electrodes of 4 human muscles. A 3-layer Daubechies4 wavelet is used to decompose surface electrodes of the muscles. The muscles include palmaris longus, brachioradialis, flexor carpi ulnaris and biceps brachii. To acquire surface electrodes, sEMG electrode-array is adhered to the skin overlying the muscles. The inputs will be classified into 5 movements, which are flexor, wrist extensor, elbow flexion, forearm pronation and forearm rotation. The movements will be modelled as output nodes. The neural network can be trained through standard BP method.

4. ASSISTIVE ROBOT CONTROL SYSTEM

4.1. QNX REAL-TIME OPERATION SYSTEM

QNX real-time platform [28–29] provides all essential functions including multi-tasking, driven by the priority scheduling and rapid pre-emptive context switching etc. The micro kernel of QNX is of small size and the minimum configuration only takes10 KB memory. The QNX real-time operating system is a micro kernel real-time operating system and it is straightforward to program the hardware interface. The QNX operating system offers four kinds of core services: process scheduling, inter-process communication, underlying network communication and interrupt handling; especially the process operates in the address space independently. The QNX minimum clock resolution can reach 10 microseconds. Within QNX, the scheduling has 32 priorities from 0 to 31 based on a first-come, first served priority policy for context switch in order to satisfy the waiting requirements for the CPU time.

At the same time, the process switch-time of QNX is very short according to the POSIX protocol API that makes it an interconnected system and convenient to implant to the UNIX/LINUX system. Therefore, QNX has been widely applied in embedded systems, robot engineering, industrial control, aerospace and other fields.

Because of the data acquisition and control of assistive robot has strong real-time requirement, PC operating system must have real-time kernel. Based on the characteristics of QNX, this paper chooses QNX as operating system platform.

4.2. ASSISTIVE ROBOT CONTROL SYSTEM

The assistive robot in the experiment system is shown in Fig. 3. The assistive robot system has three parts: sEMG system, QNX control system and the joint actuator. The assistive robot equipment is treated as a controlled plant the close loop, including the robot mechanism system, QNX system (host computer), motor driver circuits and torque sensor. The operating system of the PC is adapted as the QNX which enables the measurement, the control and the monitoring in real time. The real-time processing and communication using the network are required for the control purpose. A LAN card which has 11 Mbps transmission rate and an A/D (Analogue to Digital) converter card which has 16ch (8bit resolution) input are selected. The sensor system is used to detect the assistive robot and operator's condition and estimate the assistive force. The rotary encoder is prepared to measure the joint angle, and force sensors are installed between the two couplings. This is effective to estimate the torque generated by the EC motor.

The compliant actuation of assistive robot is compared with the theory analysis of human body's joint, a passive compliance method. A motor controlled compliant joint with a torque sensor is designed. The scheme of the assistive

robot's actuated joint system is shown in Fig. 4. The joint is for an arm joint, and has one degree of freedom. This is an experimental device for an assistive robot where restriction is imposed at the joint mobile angle to ensure user safety. Aluminium alloy and steel are used as the material of the frame in consideration of weight constraint. The actuator system of the assistive robot provides the assistive force for the arm joint. The actuator consists of an EC-motor and harmonic drive to generate the torques needed at the joint. The actuator using the harmonic drive is packed compactly with a large reduction gear ratio and smooth drive.

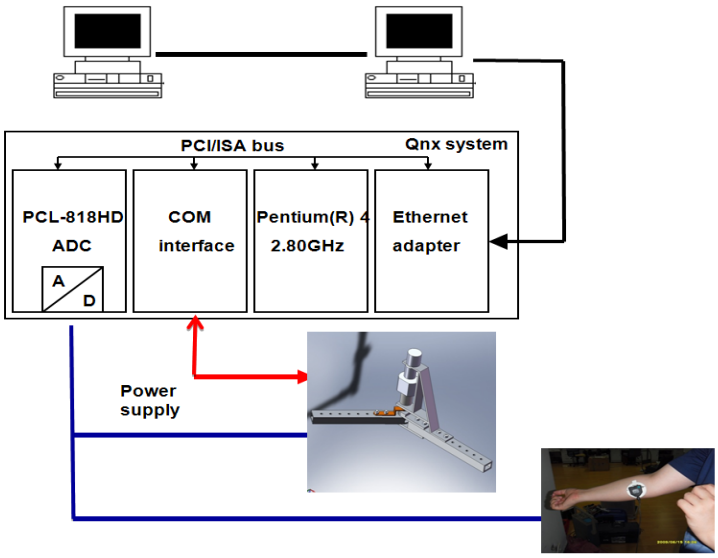

Fig. 3 – QNX system-based experimental platform for the assistive robot's compliant joint.

Fig. 4 – The experimental equipment of assistive robot.

a. *Peripheral Component Interconnection.* Peripheral Component Interconnection (PCI) is the external devices. PCI bus is located in Interconnection of microprocessor with the standard of local bus to expand the bus structure. PCI is used to bridge road connecting with local bus PCI but not directly connected with the microprocessor. In addition, PCI has good compatibility and suitable for all kinds of models, high-efficiency, obligate space for development, etc. Through the data acquisition module software can display real-time data changes and dynamic curves. In addition, the data acquisition module will write a specified file.

b. *The motor controller.* The control system uses a FAULHABER motor as the driver device. The motor controller is designed for EC micro-motor MCD2805 and with embedded encoder IE2-512. The motor can run with slow speed and the position precision of the motor can achieve 0.18. These advantages benefit that the motor is applied to robots. MCD2805 is developed from a powerful 16 bits microprocessor. The controller also has an excellent digital filter.

c. *Data Acquisition Card.* Data acquisition card adapts PCL-818HD A/D board, which contains 1K sampling FIFO buffer that can get faster data transmission and better properties. It is suitable for signal acquisition and measurement. PCL 818-HD is 16 road with single or 8 analog input, differential 12 adc sampling rate, 100KHz, 2 function switches and 11 jumpers. The software of data acquisition can be used to control. For example, the software can be used to choose analog input range, the available range of dual polarity is ±1.625V, ±1.25V, ±1.625V, ±2.5V, ±5V, ±10V and the available range of single polarity is 0–125V, 0–2.5V, 0–5V, and 0–10V.

d. *Sensor Device.* A robot system needs real-time monitoring and is to achieve joint torque accuracy requirements of experiment. This experiment platform of the sensor is abroad by HBM company T22 models of torque sensor (1D). The properties of the torque sensor is , for example, the range of torque measuring accuracy is ±5Nm, the supply voltage is 24V ac voltage and the range of output range is –5V to +5V. Then the torque signal is sampled by A/D card to transmit to PC.

5. EXPERIMENT RESULTS

5.1. TORQUE ANALYSES OF HUMAN BODY JOINT

When people move their elbow joint, the biceps muscles and triceps play an important role. The biceps muscles contract when the elbow joint flexes whilst the triceps muscles contract when the elbow joint extends [10–11]. The models and calculation formula between human muscle electromyography torque signals and surface electromyography signal can then be built as follows:

$$\tau(t) = KE(t), \tag{6}$$

where, $\tau(t)$presents the electromyography torque of biceps muscles or triceps, $E(t)$ presents surface electromyography signals, and K presents undetermined coefficient. K can be determined by measuring the difference between the measured muscle torque $\tau_m(t)$ and the estimated torque $\tau_n(t)$:

$$e(t) = \tau_m(t) - \tau_n(t). \tag{7}$$

According to the least-square method:

$$J = e^2(t) = \sum_{k=0}(\tau_m(t) - KE(t))^2, \tag{8}$$

$$\frac{dJ}{dK} = -2\sum \tau_m(t)E(t) + 2K(t)\sum E(t) = 0. \tag{9}$$

Thus

$$K = \sum \tau_m(t)E(t)/\sum E^2(t). \tag{10}$$

Put K into the equation (6), we can get the elbow electromyography torque signals.

5.2. EXPERIMENT AND ANALYSIS OF THE RESULTS

In the experiment, the surface electrodes are stuck respectively on biceps and triceps of the operator's arm. When the operator stretches the elbow up and down respectively, the experimental equipment for the assistive robot's compliant joint will follow the operator's intention accordingly. The experimental results validate the effectiveness of the design of experiments and movement intention using a trial and error method.

Through a surface electromyography amplifier circuit in the experiment, the surface electromyography of human arm biceps and triceps is measured with a data acquisition card shown as Fig. 5. The horizontal axis (x-axis) is concerned with the length of the sEMG and the vertical axis (y-axis) is concerned with the voltage. As shown in the figure, it can be seen that the property of sEMG is non-linear and the microvolt of sEMG can be amplified to the highest, 0.9 V. At the same time, the electromyography torque signal of the stretch movement and extension movement are analysed respectively. The torque is measured with the data acquisition card when the elbow joint moves.

Fig. 6a and 6b are concerned respectively with the measured torque and the estimated torque when the operator's elbow joint is flexed. Fig. 6c and 6d are concerned with the measured torque and estimated torque when the operator's elbow joint is extended. In Fig. 6a, it can be seen the value of the measured torque is negative when the operator' elbow is flexed whilst in Fig. 6b. The estimated torque is also negative accordingly. The value of the measured torque ranges from 0.8 to 1.2 Nm. In Fig. 6c, the value of the measured torque is positive when the operator'

elbow is extended whilst in Fig. 6d, it can be seen the estimated torque is also positive accordingly. The value of the measured torque ranges from 2 to 2.4 Nm. The collaboration torque curve is shown in Fig. 7 when the operator's elbow joint reciprocates. To sum up, whatever the stretch movement or extension movement is the direction of the calculated torque and measured torque is basically the same. It can be proved that the linear relationship established between sEMG and electromyography is feasible.

Then, sEMG electrode-array is secured with an adhesive interface between the skin overlying the muscle of Palmaris longus, brachioradialis, flexor carpi ulnaris and biceps brachii. The 5 movements of flexor, wrist extensor, elbow flexion, forearm pronation and forearm rotation are tested in a total of 20 data groups with a 4-channel EMG amplifier.

Comparisons have been made between various wavelets that are proved experimentally, and the Daubechies4 wavelet has been chosen. The absolute variance and the singular value of the 3-layer wavelet coefficients is extracted and used to compose 12 eigenvectors. The eigenvectors are used as input data of the neural network classifier. The input vector dimensions correspond to the testing muscle numbers multiplied by the decomposition layers, and the output vectors correspond to the number of movements.

10 training samples are chosen from each group of movements. The corresponding output node value is set to 1, and the other output node value is set to 0 which will be training as expected value. The remaining 10 groups serve as test samples. In the classification test, if one output node value is more than 0.5, it will be set to 1. At the same time the rest of output nodes are all less than 0.5, it will be set to 0. The result will be the motion patterns of the corresponding nodes.

The eigenvector extracted from wavelet coefficients and the numbers of hidden layer nodes are the two important factors that will influence the effectiveness of motion recognition. Each scale class of wavelet coefficients can constitute a matrix, and each matrix has its singular value and absolute variance which reflect the stability of the matrix. The changes of the matrix elements are small, reflecting the information and characteristics of the matrix. Therefore the singular value and absolute variance of wavelet coefficients are extracted as eigenvectors in the experiment.

If the number of nodes in hidden layer is too small, it would be impossible to fully split the feature space into multiple models. If the number of nodes in hidden layer is too large, network training will take a considerably longer time and real-time implementation may be impossible. Therefore a trade-off is necessary in determining the number of hidden layer nodes. In the experiments, 16, 14, 12 nodes in the hidden layer are selected for 500 training steps with a learning rate of 0.5.

1) With 16 nodes in the hidden layer, the average recognition rates for training and testing samples are summarised in Table 1.

Table 1

Average recognition rates
(with 16 nodes in the hidden layer)

Sample classification	Elbow flexion	Wrist flexor	Wrist extensor	Forearm pronation	Forearm rotation
Training	100%	100%	100%	100%	80%
Testing	90%	70%	100%	90%	50%

2) With 14 nodes in the hidden layer, the average recognition rates for training and testing samples are summarised in Table 2.

Table 2

Average recognition rates
(with 14 nodes in the hidden layer)

Sample classification	Elbow flexion	Wrist flexor	Wrist extensor	Forearm pronation	Forearm rotation
Training	100%	100%	100%	100%	100%
Testing	100%	100%	100%	80%	90%

3) With 12 nodes in the hidden layer, the average recognition rates for training and testing samples are summarised in Table 3.

Table 3

Average recognition rates
(with 12 nodes in the hidden layer)

Sample classification	Elbow flexion	Wrist flexor	Wrist extensor	Forearm pronation	Forearm rotation
Training	100%	100%	100%	100%	100%
Testing	100%	100%	100%	70%	80%

4) With 14 nodes in the hidden layer, the results for the singular value algorithm and absolute variance algorithm are compared in Table 4.

Table 4

Recognition rates comparison
(with 14 nodes in the hidden layer)

	Elbow flexion	**Wrist flexor**	**Wrist extensor**	**Forearm pronation**	**Forearm rotation**
Singular value algorithm	100%	100%	80%	90%	70%
Absolute variance algorithm	100%	100%	100%	80%	90%

Tables 1–3 show the number of nodes in the hidden layer has an impact on the neural network classification. When the number of hidden nodes is 14, the best movement recognition rates are achieved. The method of using wavelet coefficients to constitute feature matrix can recognise the motion accurately when an appropriate number of hidden layer nodes are chosen. Table 4 shows using the absolute variance algorithm has better recognition rate than the singular value algorithm.

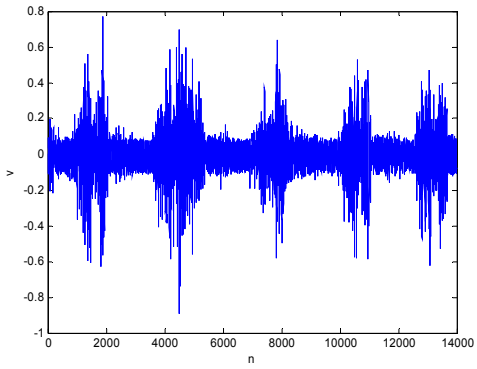

a) sEMG of biceps muscles

b) sEMG of triceps muscles

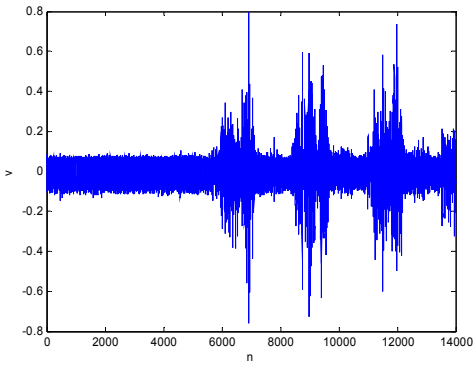

Fig. 5 – sEMG of biceps and triceps muscles when human arm elbow joint movement.

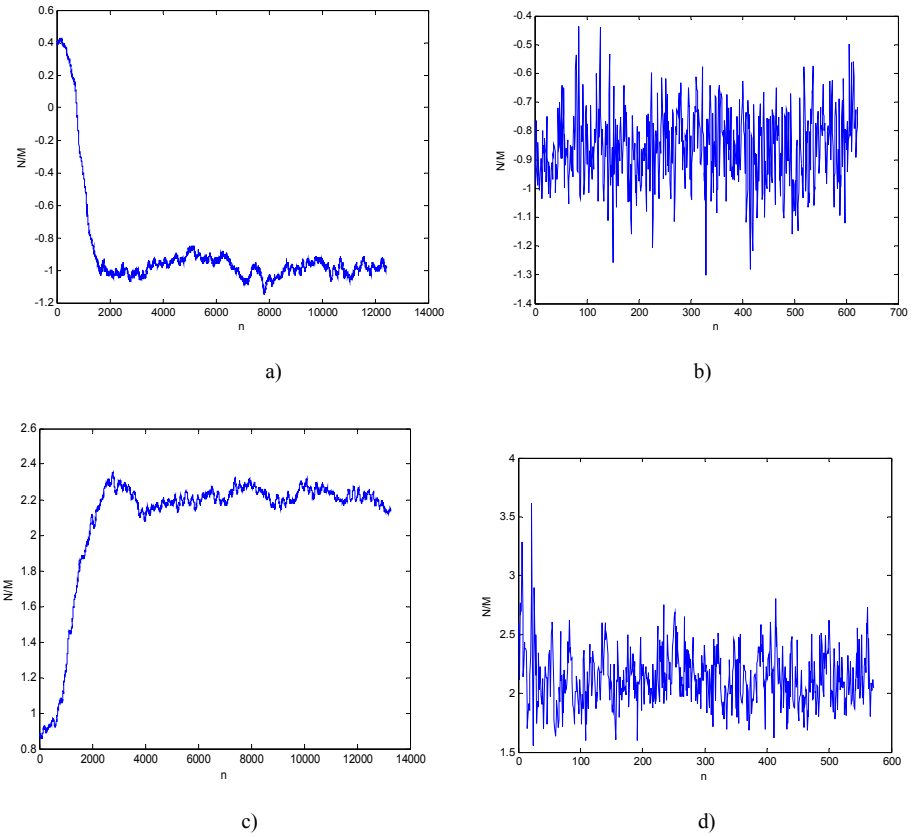

Fig. 6 – Curves of electromyography torque signals and calculated torque signals are collected when elbow joint is moving.

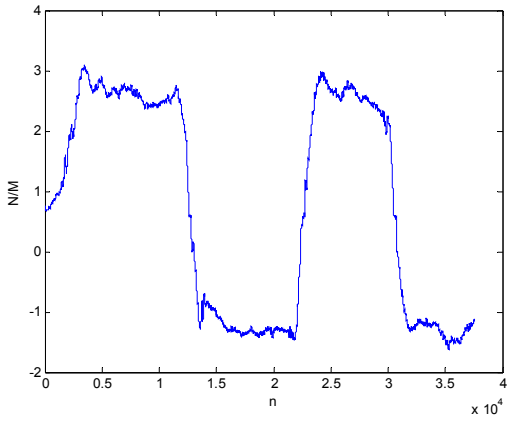

Fig. 7 – Curves of collaboration torque when elbow is reciprocating.

6. CONCLUSIONS

This paper presents a 4 channel sEMG of Palmaris longus, brachioradialis, flexor carpi ulnaris and biceps brachii with the Daubechies4 wavelet transformation. The variance of absolute value wavelet decomposition coefficients is used as signal characteristics to compose eigenvectors. The eigenvectors are used as input data of the neural network classifier to identify 5 different movement patterns of wrist flexor, wrist extensor, elbow flexion, forearm pronation and forearm rotation. This method has the advantages of a small amount of data needed, fast computation and real-time control. We have studied the sEMG acquisition method of human elbow joint related biceps and triceps muscles based on the QNX real-time operation system platform and used least-squares method to calculate models and the relationship between sEMG and electromyography torque. Experimental results verify the effectiveness and advancement of the proposed algorithm.

REFERENCES

1. Lenzi, T., De Rossi, S.M.M., Vitiello, N., and Carrozza, M.C., *Intention-based EMG control for powered exoskeletons, Biomedical Engineering*, IEEE Transactions [J], **59**, *8*, pp. 2180-2190, 2012.
2. Rinderknecht, M.D., Delaloye, F.A and Ijspeert, A.J., *Assistance using adaptive oscillators: robustness to errors in the identification of the limb parameters, Rehabilitation Robotics (ICORR)*, IEEE International Conference, 1-6, 2011.6.
3. Masafumi Okada and Shintaro Kino, *Torque transmission mechanism with nonlinear passive stiffness using mechanical singularity*, Proceeding of 2008 IEEE International Conference on Robotics and Automation, Pasadena, USA, 1735-1740, 2008.
4. Sebastian Wolf and Gerd Hirzinger, *A new variable stiffness design: matching requirements of the next robot generation*, Proceedings of 2008 IEEE International Conference on Robotics and Automation, Pasadena, USA, 1741-1746, 2008.
5. Junho Choi, Sunchul Park, Woosub Lee and Sung-Chul Kang, *Design of a robot joint with variable stiffness*, Proceeding of 2008 IEEE International Conference on Robotics and Automation, 1760-1765, 2008.
6. Dongjun Shin, Irene Sardellitti and Oussama Khatib, *A hybrid actuation approach for human-friendly robot design*, Proceedings of 2008 IEEE International Conference on Robotics and Automation, 1747-1752, 2008.
7. J.W. Hurst and A.A. Rizzi, *Series compliance for an efficient running gait*, IEEE Robotics & Automation Magazine, 42-51, 2008.
8. Vanderborght B., Verrelst B., Van Ham R. and Lefeber D., *Controlling a bipedal walking robot actuated by pleated pneumatic artificial muscles* [J], **24**, *4*, pp. 401-410, 2006.
9. Adam Zoss, H. Kazerooni and Andrew Chu, *On the mechanical design of the Berkeley lower extremity exoskeleton* (BLEEX), 2005 IEEE/RSJ International Conference on Intelligent Robots and Systems, 3132-3139, 2005.
10. Hiroaki Kawamoto and Shigehiro Kanbe, *Power assist method for HAL-3 estimating operator's intention based on motion information*, Proceedings of the 2003 IEEE International Workshop on Robots and Human Interactive Communication, 67-72, 2003.
11. Zhenbang Gong, Qinnian Wang, Zhenhua Chen and Jinwu Qian, *Robot mechanical design*, Electronics industry publicans, Beijing, China, 1995.

12. Yue H. Yin, Yuan J.Fan and Li D. Xu, *EMG and EPP-Integrated Human-Machine Interface Between the Paralyzed and Rehabilitation Exoskeleton*, IEEE Transactions on Information Technology in Biomedicine, **16**, *4*, pp. 542-549, 2012.
13. Azzerboni, G. Fincocchio, M. lpsale, *Spatio-temporal analysis of surface Electrography-signals by independent component and time-scale analysis*, Proceedings of the Second Joint EMBS/BMES Conference, **12**, *1*, pp. 112-113, 2002.
14. G. Hefftner, W. Zuccnimi and G.G. Jaros, *The electromyogram as a control signal for functional neuromuscular stimulation – Part I: autoregressive modeling as a means of EMG signature discrimination* [J/OL], IEEE Transactions on Biomedical Engineering, **35**, *4*, pp. 230-237, 1988.
15. G. Hefftner and G. Jaros, *The electromyogram as a control signal for functional neuromuscular stimulation – Part II: Practical demonstration of the EMG signature discrimination system* [J/OL], IEEE Transactions on Biomedical Engineering, **35**, *4*, pp. 238-242, 1988.
16. Dongyan Wang, Qingling Li, Zhijiang Du and Lining Sun, *Study on exoskeletal rehabilitation robot for upper limb and its control method*, Journal of Harbin Engineering University, **28**, *9*, pp. 1008-1011, 2007.
17. L. Hargrove, K. Englehart and B. Hudgins, *A comparison of surface and intramuscular myoelectric signal classification*, IEEE Transactions on Biomedical Engineering, 2007.5.
18. M. Khezri and M. Jahed, *A novel approach to recognize hand movements via SEMG Patterns*, Proceedings of the 29th Annual International Conference of the IEEE Engineering in Medicine and Biology Society, Lyon, France, 2007.
19. J. Blouin, E. Guillaud, J.P. Bresciani, M. Guerraz, and M. imoneau, *Insights into the control of arm movement during body motion as revealed by EMG analyses*, Brain Research, **1309**, pp. 40-52, 2010.
20. N. Pal and D.K. Kumar, *Classification of electromyography for localized muscle fatigue using neural networks*, Proceedings of the 7th Australian and New Zealand Intelligent Information Systems Conference, 2001, pp. 271-275.
21. Xiaowen Zhang, Yupu Yhang, Xiaoming Xu and Ming Zhang, *Wavelet based neuro-fuzzy classification for EMG control*, IEEE, 2002, pp. 1087-1089.
22. R. Begg, J. Kamruzzaman, *A comparison of neural networks and support vector machines for recognizing young-old gait patterns*, Proceedings of Conference on Convergent Technologies for Asia-Pacific Region, **1**, pp. 354-358, 2003.
23. Osamu Fukuda, Toshio Tsuji, Makoto Kaneko, Senior and Akira Otsuka, *A human-assisting manipulator teleoperated by EMG signals and arm motions*, IEEE Transactions on robotics and automation, **19**, *2*, pp. 210-222, 2003.
24. Phongchai Nilas, *A PDA-based human-robot interaction using EMG-based modified morse code*, Proceeding of the 2005 International Conference on Computational Intelligence for Modelling, Control and Automation, and International Conference Intelligent Agents, Web Technologies and Internet Commerce, 2005.
25. Wondae Ryu, Byungkil Han and Jaehyo Kim, *Continuous position control of 1 DOF manipulator using EMG signals*, Third 2008 International Conference on Convergence and Hybrid Information Technology, 2008, pp. 870-874.
26. H. Kim, B. Kang, B. Kim, and S. Park, *Estimation of multi-joint stiffness using electromyogramand artificial neural network*, IEEE Transactions on Systems, Man, and Cybernetics, Part A:Systems and Humans, **39**, *5*, pp. 972-980, 2009.
27. S.A. Mallat, *Theory for multiresolution signal decomposition: the wavelet representation*, IEEE Transactions on Pattern Analysis and Machine Intelligence, **11**, *7*, pp. 674-693, 1989.
28. ROB K, *Getting started with QNX4; A guide for real-time programmers* [J], QNX Software Systems Ltd, 1997.
29. ROB K, *TCP/IP programmer's guide*, QNX Software Systems Ltd, 1997.